

Solving the "Rotation Problem" for Closely Spaced VEP Sources



Yibin Tian¹ Shahram Dastmalchi¹ Stanley Klein¹ Thom Carney^{1,2} Justin Ales¹

¹Vision Science Group, School of Optometry, University of California, Berkeley, CA 94720

²Neurometrics Institute, Berkeley, CA 94704

Introduction

One of the challenges to functional brain imaging is to get both high spatial and temporal resolutions. Evoked potentials (EP) can provide excellent temporal resolution with relatively low cost, complementing the shortcomings of other imaging modalities. However, when multiple neural sources (modeled as dipoles) are very close in space, as occur in visual cortex, it's hard to get correct estimations of the time functions, magnitudes and locations of the activities on account of the rotation problem, whereby the same potential topology can be matched by a linear combination of different dipole time functions with an associated combination of different dipole magnitudes. Take two dipoles as an example. There are infinite pairs of time functions T_1^r & T_2^r , with associated spatial components S_1^r & S_2^r , that can generate the same scalp potential topology. The mathematical formulae are

$$V = S_1^r T_1^r + S_2^r T_2^r = S_1' T_1' + S_2' T_2'$$

$$T_2^r = -T_1 \sin(\beta) + T_2 \cos(\beta) \quad T_1^r = T_1 \cos(\alpha) + T_2 \sin(\alpha)$$

$$S_1^r = \frac{S_1 \cos(\beta) + S_2 \sin(\beta)}{\cos(\alpha - \beta)} \quad S_2^r = \frac{-S_1 \sin(\alpha) + S_2 \cos(\alpha)}{\cos(\alpha - \beta)}$$

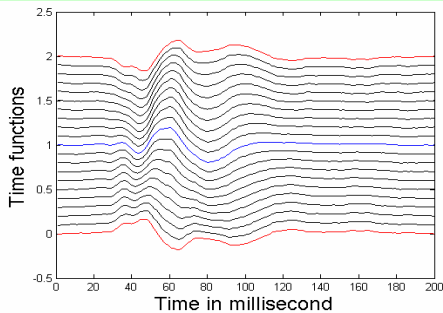


Fig.1 Time functions in the entire rotation space (step 9°)

Fig.1 shows a family of rotated time functions specified by the above equations for T_1^r or T_2^r , with the angles α or β going from 0 to 180° in steps of 9°. The top and middle curves correspond to T_1 and T_2 , the two orthogonal rotation basis functions. Any pair of these time functions, together with the associated magnitudes give identical scalp potentials.

To solve this rotation ambiguity, we have developed several new techniques for both simulations and real data. We used a large number of electrodes and a 60-patch m-sequence flickering stimulus to collect data, and utilized known human cortical anatomy and physiology to create a "ribbon metric" for data analysis. Results from both simulations and real data validate this novel approach.

Method

1 Experimental setup

A binary m-sequence modulated 60 small patches of flickering (75Hz) checkerboard stimuli (Fig.2), which was assumed to activate V1 and V2 dominantly. All 60 patches were simultaneously flickering. The m-sequence methodology allows one to find the temporal response to each individual patch by cross-correlation^[1]. 48 electrodes were densely and equidistantly put on the back of the head of two subjects who binocularly viewed the stimulus with a visual angle of 18°, mostly covering the visual cortex of interest. Because of the noisiness of the data of the inner 2 rings, only the data of the outer 4 rings (rings A, B, C and D in Fig.2) were analyzed in this study.

2 Data analysis

Berg's 4-shell spherical head model was used to calculate scalp potentials for given dipole sources (so-called forward solutions)^[2]. A nonlinear least square routine searched the possible sources (so-called inverse solutions) to predict the scalp potentials collected from the electrodes. The same time functions were used for all dipoles in the same visual cortical area corresponding to the same ring of patches in the stimulus^[3]. Dipoles in V1 and V2 corresponding to one patch of stimulus are so closely spaced that rotation ambiguity is inevitable. On the basis of the anatomy and physiology of V1 and V2, we developed "ribbon metric" to constrain the search space of the least square routine^[4]. The basic idea of "ribbon metric" is that closely spaced dipoles should have certain continuity properties with their neighbors. The metric is the weighted summation of a few sub-metrics: distance continuity metric (DCM), magnitude continuity metric (MCM) and orientation continuity metric (OCM). For each pair of time functions in the rotation space (Fig.1), the metric gives one value, which is shown as a pixel in the metric picture (Fig.3A). The minimum in the metric indicates the best solution. The weighting of the sub-metrics was determined by simulations, and the same weighting was then applied to real data.

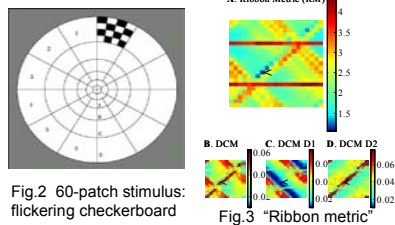


Fig.2 60-patch stimulus: flickering checkerboard

Fig.3 "Ribbon metric"

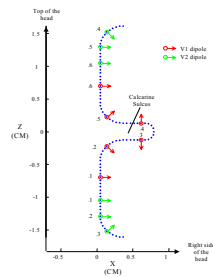


Fig.4 The half-ring dipole configuration for simulations

Results

1 Simulations

In order to validate the proposed method, scalp potentials were generated with 48 dipoles (24 in V1, 24 in V2, corresponding to 24 patches of 4 half-rings; each patch activates one dipole in V1 and V2 respectively). Dipoles for each half-ring were configured as Fig.4 (the same numbering as Fig.2), and the 4 half-rings were stacked to mimic a cortical surface (Fig.5&6, 2nd column).

For both dominant V1 dipoles and equal-magnitude V1&V2 dipoles, the following cases were simulated: no noise, white noise, correlated noise and misspecification. Misspecification refers to the distortion in the forward solutions caused by the inaccuracy of the idealized spherical head models^[5], which was simulated by adding a third far-field weak dipole to the sources in this study. These simulations all showed that the inverse solutions using "ribbon metric" are much better than those not using it. Two simulation cases are shown in Fig.5&6, where the 2nd column of surfaces are constructed from the original dipole configurations, the 3rd column reconstructed from the inverse solutions with traditional least square routine, and the 4th column from the optimal inverse solutions with "ribbon metric".

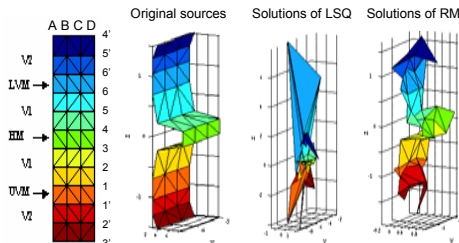


Fig.5 Locations in simulation: equal-magnitude, white noise

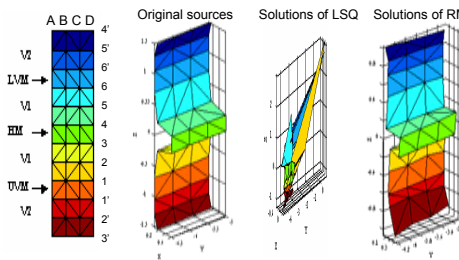


Fig.6 Locations in simulation: equal-magnitude, misspecification

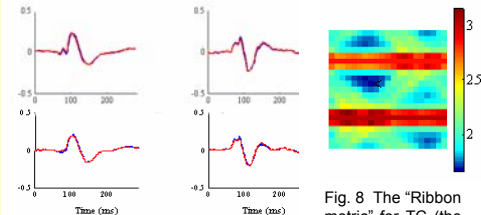


Fig.7 Time functions of V1 (left) and V2 (right) dipoles from left (blue) and right (red) hemispheres (TC, top: ring2, bottom: ring4)

Fig. 8 The "Ribbon metric" for TC (the solutions in Fig.7 correspond to the smallest value)

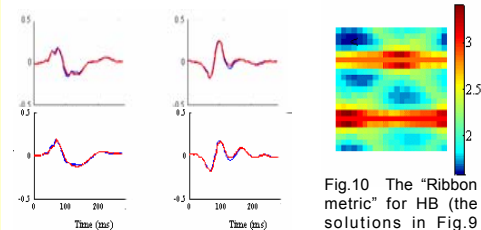


Fig.9 The same as Fig.7 for HB

Fig.10 The "Ribbon metric" for HB (the solutions in Fig.9 correspond to the smallest value)

2 Real data

The "ribbon metric" was applied to real data from two subjects (TC&HB). For each subject, dipole locations and magnitudes were localized independently with the time functions constrained to be the same around a full ring. The entire rotation space of all possible combinations of two basis time functions (the red and blue ones in Fig.1 for subject HB) was explored independently in each hemisphere, and the "ribbon metric" (Fig.8&10) was employed to pick out the best solutions. The 4 rings were allowed to have different time functions. For the same ring, the time functions for V1 and V2 dipoles from left and right hemispheres were compared; they are very similar in all 4 rings in both subjects (ring2 and ring 4 are shown in Fig.7&9). This similarity provides strong evidences validating the proposed method. Further validation of the locations and magnitudes using information from functional magnetic resonance imaging (fMRI) is under investigation.

References

- [1] Sutter, Nonlinear vision, 171-220, 1992.
- [2] Berg & Scherg, EEG and clinical neurophysiology, 90: 58-64 1994.
- [3] Slotnick & Klein et al, Clinical neurophysiology, 110: 1793-1800, 1999.
- [4] Dastmalchi, PhD thesis, Ch2, UC Berkeley, 2003.
- [5] Zhang & Jewett et al, Brain topography, 17: 151-161, 1994.